

Switchable Water-Adhesive, Superhydrophobic Palladium-Layered Silicon Nanowires Potentiate the Angiogenic Efficacy of Human Stem Cell Spheroids

Jungmok Seo, Jung Seung Lee, Kihong Lee, Dayeong Kim, Kisuk Yang, Sera Shin, Chandreswar Mahata, Hwae Bong Jung, Wooyoung Lee, Seung-Woo Cho,* and Taeyoon Lee*

Three-dimensional (3D) cell spheroids have great potential for cell therapy and tissue engineering due to their therapeutic and regenerative capacity.^[1] Spheroids mimic an *in vivo* 3D microenvironment through cell-cell and cell-matrix interactions, allowing cells in 3D spheroids to exhibit improved proliferation, differentiation, and cellular function compared to cells grown in two-dimensional (2D) culture.^[1g,2] In fact, several studies report the therapeutic efficacy of spheroids prepared from various types of cells including endothelial cells, hepatocytes, neural stem cells, and mesenchymal stem cells.^[1f,1g,2c,3] Methods including hanging drop on the typical culture dishes and suspension culture in spinner flask and microwell have been applied to produce cell spheroids for therapeutic applications.^[2c,4] However, the viability,^[5] uniformity,^[4c] and functionality^[6] of spheroids generated by conventional methods need improvement. To produce spheroids of sufficient quality for therapeutic applications, it is essential to use culture substrates capable of minimizing cell adhesion to the substrates while facilitating cell-cell and cell-extracellular matrix (ECM) interactions. Therefore, hydrophobic surfaces have been developed to meet these surface characteristics, but they are often inefficient in spheroid formation due to excess cell adhesion on the surfaces during spheroid culture and also have challenges in manufacturing to fabricate the surfaces.^[4a,7]

Nature-inspired superhydrophobic surfaces with special wetting and adhesion properties have gained attention due to their potential for biological applications.^[8] In particular, reversible superhydrophobic adhesion switching between water adhesive and water repellent properties is highly desirable for more efficient hanging drop spheroid culture because it allows for surface binding of medium droplets and induces subsequent recovery of superhydrophobic properties on sites without droplet contact. This may lead to formation and maintenance of compact spherical droplets on the surfaces, which facilitates minimizing of interactions between liquid and substrates. Such reversible switching of superhydrophobic adhesion properties can be achieved by adjusting surface chemical and physical properties,^[9] that are reversibly sensitive to external stimuli including temperature,^[10] magnetic field,^[11] ultraviolet irradiation,^[10b,12] and pH.^[13] However, these stimuli-induced reversible transitions take longer than a few minutes to achieve and hydrophilic domains are often generated in the process, which results in failure to maintain the spherical shape of aqueous droplets on the surface during the hanging drop culture. Therefore, more efficient culture of high quality cell spheroids might be achieved by developing superhydrophobic surfaces with efficient, rapid switching water adhesion properties.

In this study, we report a novel and facile strategy to potentiate the therapeutic efficacy of 3D stem cell spheroids using bio-inspired superhydrophobic surfaces with switchable water adhesion properties. The water-adhesion switchable superhydrophobic surface was fabricated by deposition of a gas-sensitive palladium (Pd) layer onto vertically aligned silicon (Si) nanowires (NWs) and by subsequent coating with dodecylalkyltrichlorosilane (DTS). The resulting Pd-covered Si NWs (Pd/Si NWs) exhibit high water-repellant properties under atmospheric conditions. The surface of the Pd/Si NWs becomes water adhesive when exposed to ambient hydrogen (H₂). The adhesion transition process occurred within only 5 seconds and the Pd/Si NWs showed extremely large water contact angle (WCA) (>150°) in both ambient. A precisely controlled volume of culture medium with cells can be captured onto the H₂-exposed Pd/Si NWs and size-controlled human adipose-derived stem cell (hADSC) spheroids can be obtained through hanging-drop culture. The paracrine ability of hADSC spheroids can also be controlled by optimizing the number of seeded cells. Compared to spheroids formed by conventional methods (spinner flask suspension culture and hanging drop culture on a petri dish), hADSC spheroids produced on the Pd/Si NWs exhibited more uniform

Dr. J. Seo, D. Kim, S. Shin, Dr. C. Mahata, Prof. T. Lee
Nanobio Device Laboratory
School of Electrical and Electronic Engineering
Yonsei University
50 Yonsei-ro
Seodaemun-Gu, Seoul 120-749, Republic of Korea
E-mail: taeyoon.lee@yonsei.ac.kr



J. S. Lee, K. Lee, K. Yang, Prof. S.-W. Cho
Stem Cell and Biomaterial Engineering Laboratory
Department of Biotechnology
Yonsei University
50 Yonsei-ro
Seodaemun-Gu, Seoul 120-749, Republic of Korea
E-mail: seungwoocho@yonsei.ac.kr

H. B. Jung, Prof. W. Lee
Nano Device Laboratory
Department of Materials Science and Engineering
Yonsei University
50 Yonsei-ro
Seodaemun-gu, Seoul 120-749, Republic of Korea

DOI: 10.1002/adma.201402273

size distribution and significantly enhanced vascular endothelial growth factor (VEGF) secretion. Hanging-drop culture of hADSCs on Pd/Si NWs promoted cell-cell interaction and ECM production, which improved cell viability and reduced apoptosis. Most importantly, the conditioned medium from hADSC spheroid culture on Pd/Si NWs significantly enhanced proliferation and capillary formation of human umbilical vein endothelial cells (HUVECs) under simulated ischemia and in normoxia. Our current study demonstrates that water-adhesive superhydrophobic surfaces augment the angiogenic potential of human stem cell spheroids. To the best of our knowledge, this is the first attempt to obtain 3D stem cell spheroids with enhanced functionality on a water adhesion switchable superhydrophobic surface.

The bio-inspired superhydrophobic surface with switchable water adhesion properties was fabricated as described in our previous work.^[14] Vertically aligned Pd/Si NWs were obtained via aqueous electroless etching (AEE) of Si, followed by sputter deposition of a gas-sensitive Pd layer. As shown in Figure S1, the fabricated Pd/Si NWs were vertically aligned over a large

area and were uniform in length. The tips of Pd/Si NWs were locally bundled with the micrometer scale clusters. The inter-distance between individual Si NWs in the cluster was estimated to be in the nanometer scale range. It is believed that poor step coverage of sputtering resulted in Pd atoms not reaching the roots of the Si NWs, therefore, the deposited Pd layer was predominately formed at the tips of the Si NWs.

The deposited Pd layer induces morphological change on the Pd/Si NWs, which generates a water pinning force between the water droplet and the surface of the Pd/Si NW. Figure 1a and b show schematic illustrations of the volumetric changes that occur in Pd/Si NWs under ambient air and hydrogen, respectively. Pd is a well-known hydrogen sensitive material because Pd easily dissolves hydrogen, forming nonstoichiometric hydrides of general composition similar to other transition and rare-earth metals.^[15] At air ambient, the Pd atoms are in the form of a three-dimensional periodic fcc structure with a lattice constant of 3.90 Å. When the Pd/Si NWs are exposed to H₂, hydrogen molecules are adsorbed onto the Pd layer. The adsorbed hydrogen molecules are dissociated into

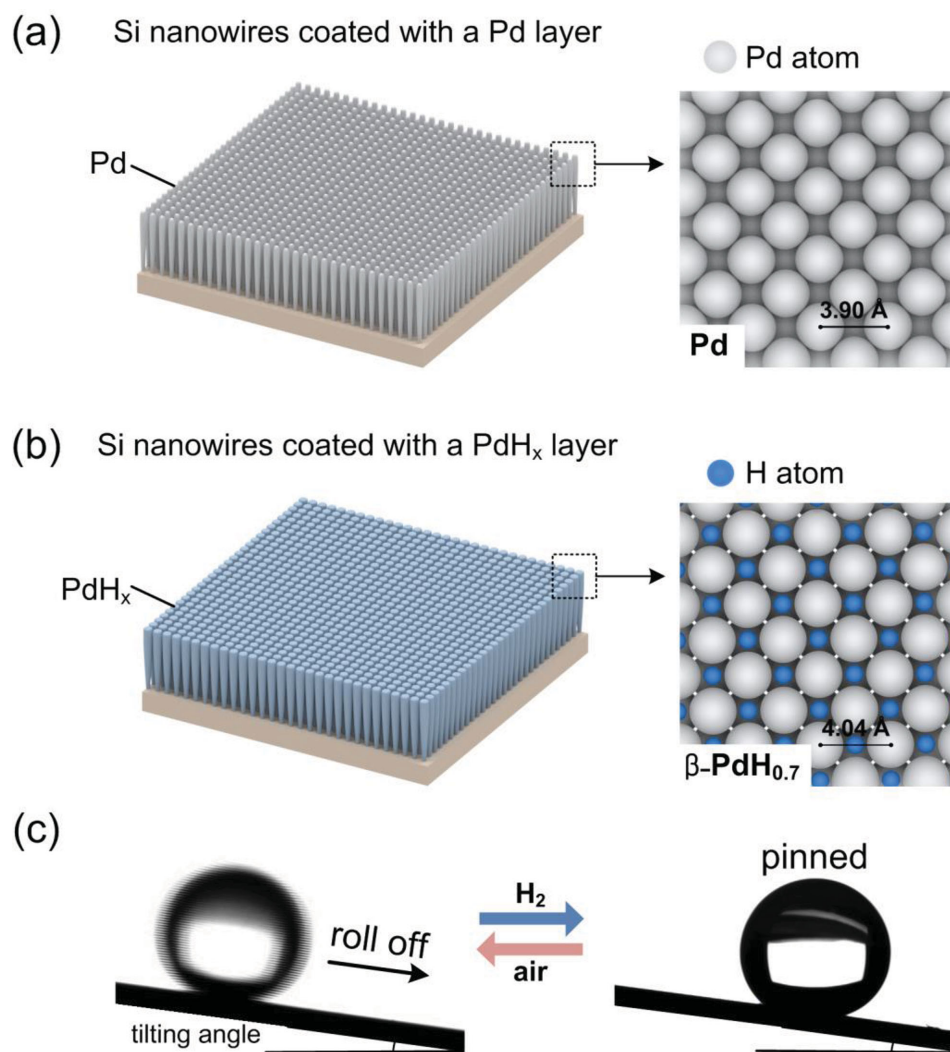


Figure 1. The schematic illustrates H₂-induced Pd/Si NW surface structural change and volume change under ambient a) air and b) H₂. c) Images show water droplets on Pd/Si NW surfaces tilted at 5° under ambient atmosphere (left) and H₂ (right).

single hydrogen atoms, which diffuse and react with Pd atoms resulting in the formation of β -phase Pd hydride (PdH_x). In PdH_x , the hydrogen atoms occupy the octahedral interstitial sites of the Pd lattice and filling of the interstitial sites by hydrogen atoms causes a volumetric expansion of the lattice constant from 3.90 to 4.04 Å (Figure 1a and b). The expanded volume of the Pd layer can be restored to its initial volume under ambient air due to phase transition of PdH_x to Pd. These reversible volume changes of the covered Pd layer result in changes to the geometrical structure of Pd/Si NWs, which strongly relates to alteration in water adhesion energy of the superhydrophobic surface.

Figure 1c shows superhydrophobic adhesion switching of the Pd/Si NWs. At ambient atmospheric conditions, 8 μl of water droplet can roll off of the surface when the surface is slightly tilted or even horizontal (without intentionally tilting the sample), which indicates the extreme water-repellant properties of Pd/Si NW arrays (left image Figure 1c). After exposure to 8% H_2 , water adhesion properties of the Pd/Si NWs instantly and dramatically switch from being water repellent to water adhesive (right image Figure 1c). Water repellent properties can be restored when the substrate is placed back in ambient air. Figure S2a and b are typical images of static WCA on the Pd/Si NWs at ambient air and H_2 , respectively. The measured WCA of the Pd/Si NWs slightly decreased from $158.4 \pm 3.37^\circ$ to $153 \pm 3.58^\circ$ when the surface was exposed to H_2 ; however, the surface showed superhydrophobic properties in both ambient conditions. As shown in Figure S2c, the adhesion switching process can be repeated for several cycles, indicating the sustainable reversibility of gas-driven water adhesion switching of Pd/Si NWs. Notably, DTS coating on the Pd/Si NWs to obtain superhydrophobic properties does not significantly affect water adhesion switching of Pd/Si NWs, as shown in our previous study.^[14]

Theoretically, the superhydrophobicity of Pd/Si NWs is similar to the Cassie-Baxter wetting model. The Cassie-Baxter model assumes that water droplets on a surface sit on air cushions between the droplet and the rough surface, which results in very low contact angle hysteresis.^[16] In this model, water adhesion energy can be determined by the actual contact area between the surface and the water droplet. According to a previous report that investigated dynamic droplet adhesion on superhydrophobic surfaces using the Cassie-Baxter model, water adhesion energy can be enhanced by the increment of the engineered micro and nano-pillar structure perimeters.^[17] Therefore, the increment of water adhesion energy under ambient H_2 could be explained by the enlarged size of the clustered Pd/Si NWs due to volume expansion of the Pd layer.

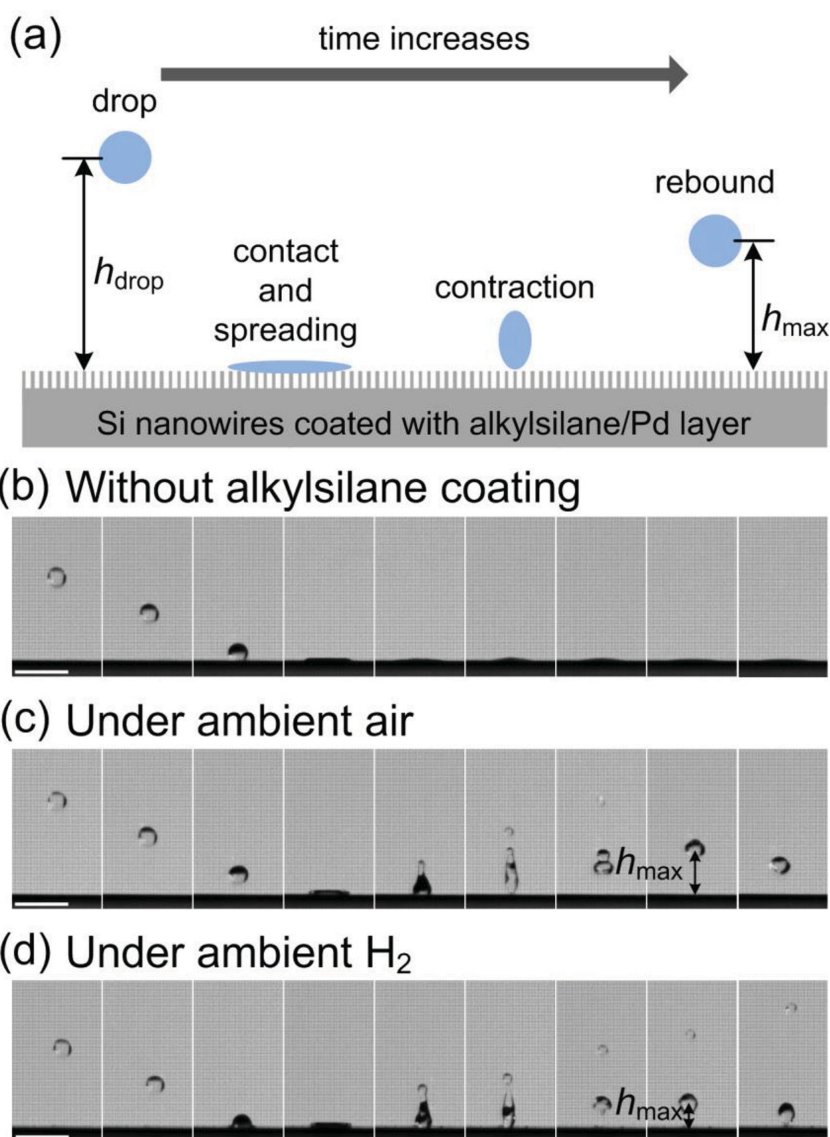


Figure 2. The schematic illustrates a) the dynamic behavior during collision of a water droplet onto the Pd/Si NW surface. Chronological images show the falling water droplet on the Pd/Si NW surface b) without DTS coating, c) under ambient air, and d) under ambient H_2 . Scale bars indicate 5 mm.

To obtain the water adhesion energy of the Pd/Si NWs, the impact of water droplet dynamics on the surface was investigated. The water adhesion energy of the superhydrophobic surface can be calculated using the law of energy conservation.^[18] Figure 2a depicts the dynamic bouncing behavior of a water droplet on the superhydrophobic surface. During the impact and bouncing process, surface adhesion-induced energy loss (E_{loss}) occurs and can be calculated by the difference in potential energy as follows:

$$E_{\text{loss}} = \rho V g (h_{\text{drop}} - h_{\text{max}}) \quad (1)$$

where ρ is the water density, V is the droplet volume, g is the gravitational acceleration constant, h_{drop} is the initial height of the water droplet, and h_{max} is the maximum height of the

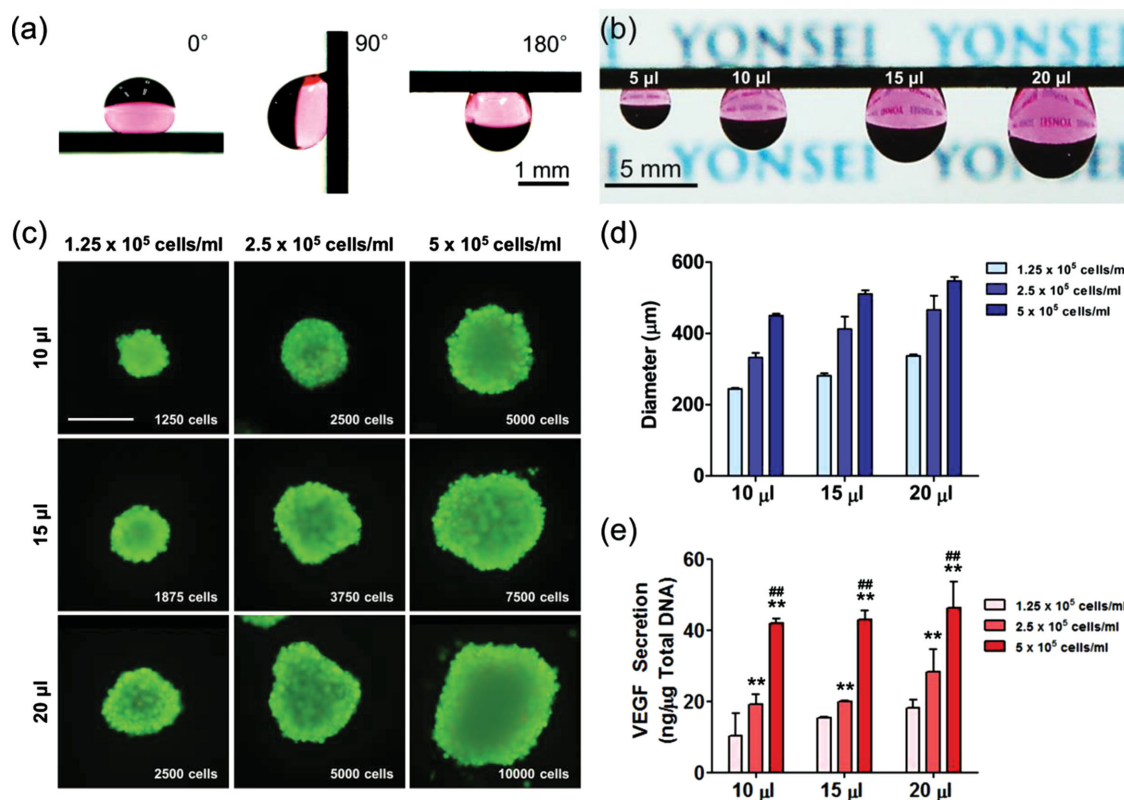


Figure 3. The images show a) culture medium droplets adhered on the H₂-exposed Pd/Si NWs with substrates tilted at 0°, 90°, and 180° (from left to right). b) Cell culture medium droplets containing precisely controlled volumes are shown on the H₂-exposed Pd/Si NWs in hanging-drop position. Size and paracrine secretion in hADSC spheroids is controlled. c) Live/Dead staining was performed in spheroids after 4 days of culture at different cell densities (1.25, 2.5, and 5.0 × 10⁵ cells/ml) and in differing medium volumes (10, 15, and 20 μl), scale bar = 500 μm. d) The size distribution of the spheroids is shown (n = 4). e) VEGF protein secreted from the spheroids was quantified using an ELISA (n = 3, **: p < 0.01 compared to the density of 1.25 × 10⁵ cells/ml, ##: p < 0.01 compared to the density of 2.5 × 10⁵ cells/ml).

bounced droplet. Figure 2b shows sequential images (obtained using a high-speed camera with a 6-ms scan speed) of an 8-μl water droplet impinging on the superhydrophilic Pd/Si NW surface without the DTS coating layer. The initial height (h_{drop}) was maintained at 5.3 cm. The water droplet did not bounce or spread out along the surface; this indicates that the Pd/Si NW surface without a DTS coating was superhydrophilic. The Pd/Si NW surface became superhydrophobic with extreme water repellent properties after DTS coating. As shown in Figure 2c, the water droplet appeared to bounce off of the Pd/Si NW without penetrating the nanostructure, which can be attributed to an air cushion supporting the water droplet upon impact. A similar bouncing behavior was observed on the Pd/Si NW after exposure to H₂ (Figure 2d). However, in this instance, h_{max} was decreased due to increased water adhesion of the Pd/Si NW. Notably, during the impinging and rebounding process, water droplets get highly elongated after impacting both superhydrophobic surfaces and emit a small satellite droplet. The deformations of the impinging water droplet are closely related to the Weber number ($W_e = \rho S^2 R / \gamma$, where S is the impact speed, R is the droplet diameter, and γ is the liquid surface tension). In both case, the shape of the deformation was almost same since the experimental conditions which affect to the W_e were fixed during the experiments. Therefore, the separation of the bouncing droplet does not significantly affect to the potential

energy difference and E_{loss} . By using 72.8 mN/m as the surface tension for water and 9.8 m/s² as g , the generated adhesion energy can be calculated to determine the difference in energy loss between ambient air and H₂. After excluding other causes of energy loss including friction between air and water, we determined that the adhesion energy (E_{adh}) of the Pd/Si NWs was 161 nJ.

Due to the increased adhesion energy of Pd/Si NWs after exposure to H₂, the surface water adhesion properties was changed dramatically and precisely controlled volume of droplets can be adhered without further patterning processing. Figure 3a shows images of a 10-μl droplet of aqueous cell culture medium adhering onto H₂-exposed Pd/Si NWs. The droplets were adhered onto the surface right after the exposure of H₂ and maintained under ambient air. The droplet was firmly pinned to the surface, even when the substrate was tilted vertically or turned upside down. Figure 3b shows adhered cell culture medium at varying volumes, 5 to 20 μl, on the Pd/Si NWs. At volumes larger than 20 μl, the pinned water droplet rolled off because the water-adhesion energy was not high enough to hold more than 20 μl of water in place (data not shown).

The water adhesion switch properties of Pd/Si NWs could be directly applied to 3D spheroid formation using the hanging drop method. To test the feasibility of using this platform for stem cell spheroid formation, hADSC spheroids were

generated on Pd/Si NWs and analyzed those cells after 4 days culture. Viability of spheroids was maintained on Pd/Si NWs during culture (Figure 3c). Spheroid size increased proportionally to the seeding density and media volume (Figure 3c and d). VEGF secretion from hADSC spheroids (normalized to total DNA content in each group) was depended on spheroid size (Figure 3e), which indicates that hADSC spheroids can be engineered to have enhanced paracrine activity by adjusting cell density and culture medium volume.

It should be pointed out that water adhesion switchable surface hinders the spreading out of water droplet during the entire period of cell culture. On the Pd/Si NWs, the surface region lacking direct contact with the droplets becomes water repellent again within a minute due to the fast, reversible switching property. Therefore, the wettability switching-induced strong hydrodynamic resistance to spreading can be generated at the liquid-substrate contact interface as a water repellent superhydrophobic area surrounds the droplet contact area. Accordingly, spreading of the adhered droplet can be minimized and the adhered droplet can be maintained in a nearly spherical form on the substrate during the spheroid formation.

On the conventional water adhesive superhydrophobic surfaces without switching property, water droplets can also be firmly pinned to the surface even when the substrate is turned upside down. However, unlike the Pd/Si NWs, the wetting switching-induced hydrodynamic resistance cannot be generated on the water adhesive superhydrophobic surfaces, due to unchanged surface structures and/or chemical properties.^[19] Consequently, the adhered water droplets on such conventional water adhesive superhydrophobic surfaces tend to spread out more readily and do not retain their spherical shape on the surfaces. Thus, we believe that our water adhesion switchable surface may be more suitable for the hanging droplet culture allowing minimized spreading of cell culture medium during the spheroid formation.

hADSC spheroid size and paracrine activity on the Pd/Si NWs were compared with spheroids produced by conventional methods (suspension culture in spinner flask and hanging-drop culture on a petri dish). As shown in Figure 4a and b, hADSCs grown on Pd/Si NWs produced more viable, compact spheroids with a narrow size distribution compared to those grown with spinner flask and petri dish methods. Moreover,

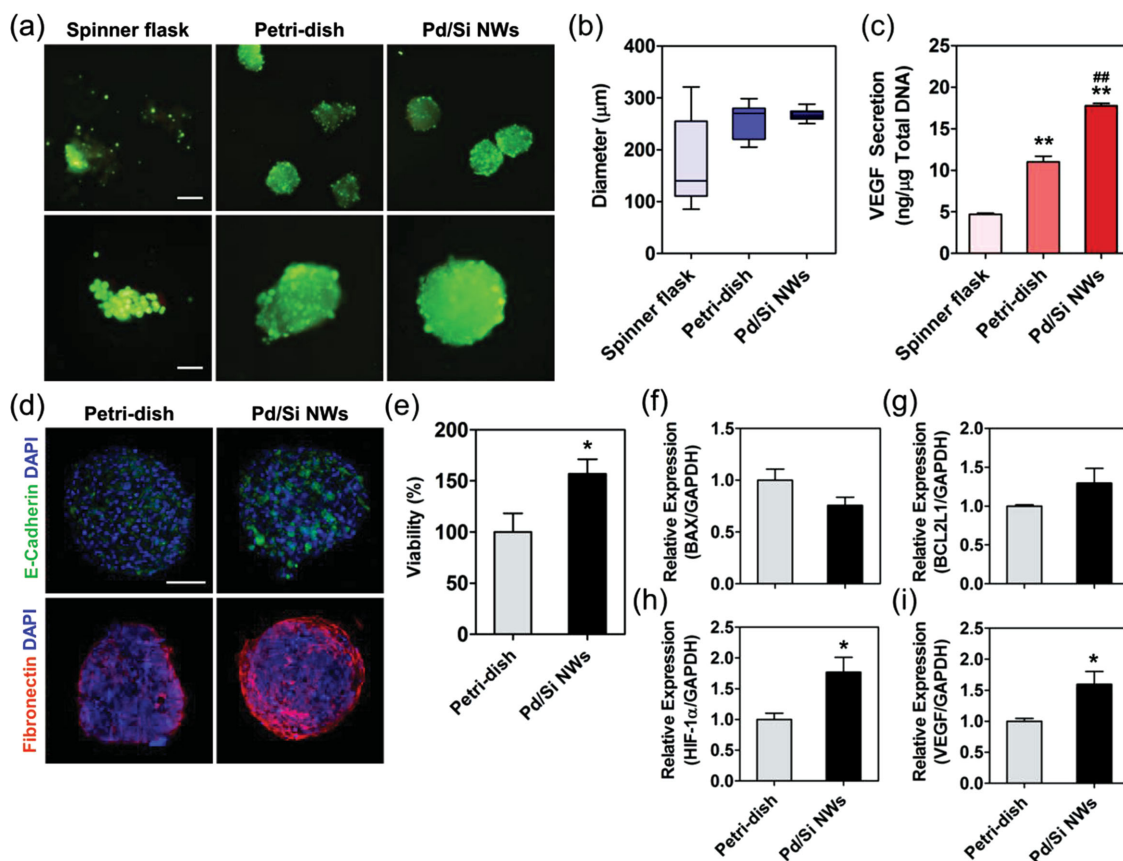


Figure 4. a) Live/Dead staining was performed on hADSC spheroids generated from spinner flask, petri dishes, and Pd/Si NWs after 4 days in culture, scale bars = 250 μm (upper) and 100 μm (lower). b) The size distribution of spheroids is shown ($n = 10$). c) VEGF protein secreted from the spheroids was quantified ($n = 3$, **: $p < 0.01$ compared to the spinner flask group, #: $p < 0.01$ compared to the petri dish group). d) Spheroids were stained with immunofluorescence for E-cadherin and fibronectin, scale bar = 100 μm . e) Mitochondrial metabolic activity of the spheroids was measured by MTT assay ($n = 5$, *: $p < 0.05$ compared to the petri dish group). The metabolic activity of the Pd/Si NW group was normalized to that of the petri dish group. qRT-PCR was used to quantify the level of expression of f) BAX, g) BCL2L1, h) HIF-1 α , and i) VEGF ($n = 3$, *: $p < 0.05$ compared to the petri dish group). Gene expression in the Pd/Si NW group was normalized to that of the petri dish group.

the level of VEGF secretion was much greater from hADSC spheroids formed on Pd/Si NWs than from those produced in spinner flasks and petri dishes (Figure 4c). These results indicate that Pd/Si NWs can be used to produce functional human stem cell spheroid cultures with high metabolic activity and uniform size.

Hanging-drop culture of hADSCs on Pd/Si NWs enhanced cell proliferation and reduced apoptosis by promoting cell-cell and cell-matrix interaction. To investigate the potential mechanism responsible for improved viability and paracrine secretion, mitochondrial metabolic activity, apoptosis signaling, and ECM production were examined in hADSC spheroids formed on Pd/Si NWs versus petri dishes. In these tests, the spinner flask group was excluded because the spheroids generated in a spinner flask show low viability and low levels of VEGF secretion. Immunocytochemical staining of hADSC spheroids revealed that expression of the cell-cell junction protein E-cadherin and ECM protein fibronectin was higher in hADSC spheroids on the Pd/Si NWs than in those on petri dishes (Figure 4d). This indicates that Pd/Si NWs enhance cell-cell and cell-matrix interaction in spheroids. Mitochondrial metabolic activity was examined in the spheroids by 3-(4,5-dimethylthiazol-2-yl)-2,5-diphenyltetrazolium bromide (MTT) assay. Activity was much higher ($p < 0.05$) in spheroids cultured on the Pd/Si NWs than in those on petri dishes (Figure 4e). Quantitative real-time polymerase chain reaction (qRT-PCR) analyses indicated that gene expression of pro-apoptotic factor BCL2-associated X protein (BAX) and anti-apoptotic molecule BCL2-like 1 (BCL2L1) was downregulated and upregulated, respectively, in spheroids cultured on Pd/Si NWs compared to those on petri dishes (Figure 4f and g). These results demonstrate that water-adhesive superhydrophobic Pd/Si NWs can reinforce cell-cell and cell-matrix interactions by inducing formation of highly compact spheroids, which ultimately enhances stem cell metabolic activity and proliferation and reduces apoptosis during spheroid culture.

The observed enhanced viability and VEGF secretion could be further explained by metabolic adaptation of hADSCs in response to hypoxic conditions created in the spheroids. When a hypoxic microenvironment is generated within the spheroids, the cells in the central part of the spheroids typically undergo apoptosis due to diffusion limitations of oxygen and nutrients to the hypoxic core. This results in decreased viability and metabolic activity of stem cells in the spheroids.^[20] However, hypoxic adaptation supports cells within the spheroids to retain their viability and function. The expression of hypoxia-inducible factor-1 α (HIF-1 α), a transcriptional factor that responds to hypoxia, was significantly upregulated ($p < 0.05$) in hADSC spheroids grown on Pd/Si NWs compared to those cultured on petri dishes (Figure 4h). This may be due probably to alteration in oxygen metabolic signalling resulting from the enhanced cell-cell and cell-matrix interaction in highly compact hADSC spheroids formed on the Pd/Si NWs.^[21] Upregulated expression of HIF-1 α in response to hypoxia is known to stimulate signal transduction of a wide spectrum of anti-apoptotic^[22] and angiogenic growth factors including VEGF, insulin-like growth factor-2,^[23] and basic fibroblast growth factor.^[24] Thus, hanging-drop culture on Pd/Si NWs can induce metabolic adaptation of hADSCs in spheroids exposed to hypoxia and it can improve

cell survival in hypoxic conditions.^[1g,2c] qRT-PCR analyses showed that VEGF gene expression was upregulated ($p < 0.05$) on the Pd/Si NWs (Figure 4i), which is consistent with enzyme-linked immunosorbent assay (ELISA) data indicating that increased VEGF secretion occurs in spheroids grown on Pd/Si NWs (Figure 4c).

We evaluated the angiogenic potential of hADSC spheroids formed on Pd/Si NWs by examining proliferation and capillary formation of human endothelial cells cultured with conditioned medium obtained from hADSC spheroid culture. The conditioned medium from each spheroid group (spinner flask, petri dish, and Pd/Si NWs) was collected after 4 days of spheroid culture and HUVECs were cultured with the conditioned medium under either normal conditions (normoxia; 20% O₂ content) or simulated ischemic conditions (hypoxia; 1% O₂ content). Endothelial growth medium-2 (EGM-2) and endothelial basal medium (EBM) served as a positive and negative control, respectively. The conditioned medium from the Pd/Si NWs group significantly enhanced HUVEC proliferation under both normal (Figure 5a) and hypoxic conditions (Figure 5b) compared to medium from spheroids grown in spinner flasks and petri dishes. In addition, conditioned medium from hADSC spheroid culture on Pd/Si NWs significantly accelerated capillary formation of HUVECs 5 hours after plating on Matrigel (Figure 5c). The capillary density was much higher in the Pd/Si NW-conditioned medium group than in the other conditioned medium groups (Figure 5d). The ability of the Pd/Si NW-conditioned medium to induce capillary formation was comparable to that of EGM-2 medium supplemented with growth factors and serum (Figure 5d). These results indicate that the angiogenic efficacy of hADSC spheroids can be potentiated through hanging-drop culture on Pd/Si NWs, likely due to increased paracrine secretion of factors such as VEGF.

Quality control of spheroid formation depending on the surface types for hanging-drop culture can be explained by differential internal hydrodynamic flow of the medium during the spheroid formation, as shown in Figure 6.^[25] Internal flow of the static hanging droplet can be affected by various factors including chemical properties of the medium and surfaces, geometrical structures of the surfaces, and by the evaporation rate of the medium. The contact line of the medium to surface, on both the petri dish and Pd/Si NW surface, was pinned and the area of the medium to surface remained almost constant during spheroid formation. In the pinned contact mode, the outward hydrodynamic flow is generated toward the periphery to compensate for the loss of medium near the contact line. Therefore, cell aggregates can be localized at the contact line. As the size of aggregates increases, the gravity force exerted on the aggregates can exceed the internal hydrodynamic force, and the aggregates form spheroids at the drop apex. The horizontal hydrodynamic flow on the petri dish surface is much stronger than that on the Pd/Si NW surface due to the relatively small contact angle and large contact area (Figure 6a). Consequently, aggregated cells may more readily accumulate at the droplet apex on Pd/Si NWs, resulting in generation of more compact and functionally improved hADSC spheroids (Figure 6b).

In summary, we demonstrate a bio-inspired, facile approach to generate functional 3D human stem cell spheroids using switchable water-adhesive, superhydrophobic surfaces.

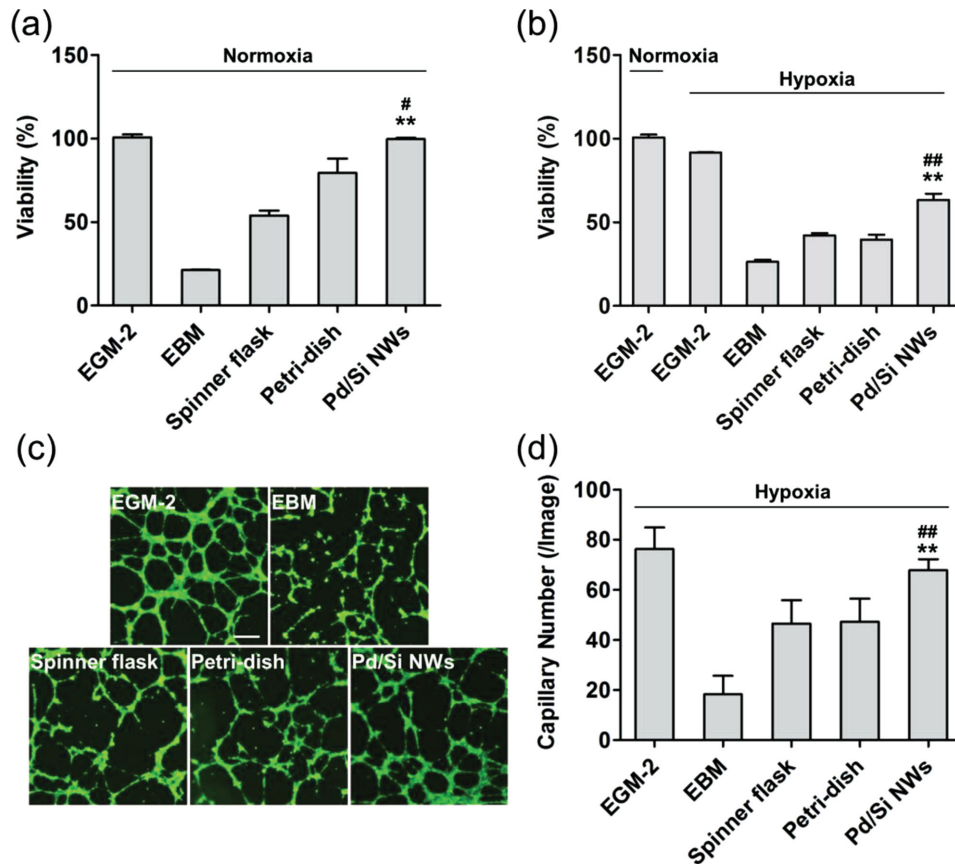


Figure 5. An in vitro functional assay of HUVECs was performed using conditioned medium from hADSC spheroid culture. HUVECs were cultured in EGM-2 (with growth factors and serum supplementation), EBM (without growth factors and serum supplementation), and mixed medium containing EBM and the conditioned medium at a volume ratio of 7:3. After 2 days in culture, the viability of HUVECs cultured in a) normoxic (20% oxygen) and b) hypoxic (1% oxygen) conditions was evaluated using MTT assay ($n = 3$, **: $p < 0.01$ compared to the spinner flask group, # & ##: $p < 0.05$ & 0.01 , respectively, compared to the petri dish group). The viability of each group was normalized to that of the EGM-2 group. c) Capillary formation by HUVECs under hypoxic (1% oxygen) conditions was visualized by calcein-AM staining 5 hours after plating on Matrigel. d) The number of capillaries (per image) was counted ($n = 4$, **: $p < 0.01$ compared to the spinner flask group, ##: $p < 0.01$ compared to the petri dish group).

The fabricated superhydrophobic Pd/Si NW surface has both highly water repellent properties and water adhesive properties, and adhesion characteristics can be switched quickly and reversibly by ambient gas. Reversible superhydrophobic adhesion switching is based on rapid absorption and desorption of

H atoms into the Pd lattice structure that results in subsequent morphological changes to the Pd/Si NWs. The Pd/Si NW surface enables hanging-drop culture to produce human stem cell spheroids with uniform size distribution and enhanced angiogenic potentials compared to the conventional spheroid culture

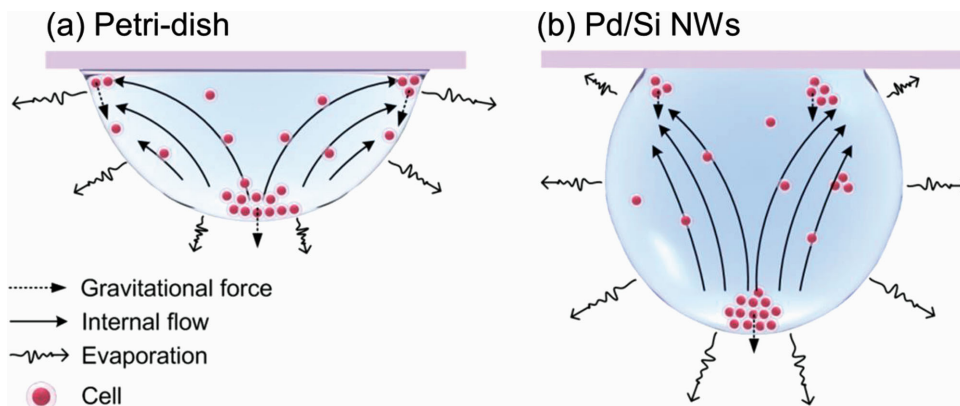


Figure 6. The schematic represents the internal hydrodynamic flow in the cell culture medium drop during formation of 3D stem cell spheroids. Hydrodynamic flow is shown in a hanging droplet on a a) petri dish and b) Pd/Si NW.

methods. Reduced horizontal hydrodynamic flow in droplets on the Pd/Si NWs generates high quality stem cell spheroids, likely due to compact spheroid formation with extensive cell-cell and cell-matrix interactions. The potentiated ADSC therapy via spheroid culture on the Pd/Si NWs can be applied for the treatment of various ischemic diseases such as ischemic stroke, myocardial infarction, and hindlimb ischemia. The efficacy of the spheroids for therapeutic angiogenesis in vivo would be examined in future studies. Spheroid culture using Pd/Si NW surfaces should also be scaled-up and further optimized for mass production of the functional ADSC spheroids for the therapeutic purpose.

Supporting Information

Supporting Information is available from the Wiley Online Library and from the author.

Acknowledgements

Jungmok Seo and Jung Seung Lee contributed equally to this work. This research was supported by the Priority Research Centers Program (2012-0006689) through the National Research Foundation (NRF) of Korea funded by the Ministry of Education, Science and Technology (MEST), by the NRF grant funded by the Korean government (MEST) (No. 2011-0028594), by a grant (2010-0020409) from the NRF funded by the Ministry of Science, ICT, and Future Planning (MSIP), Republic of Korea. This work was also supported by a grant (2009-0083522) from the Translational Research Center for Protein Function Control (TRCP) funded by the MSIP, Republic of Korea, and the Industrial strategic technology development program (10041041) funded by the Ministry of Knowledge Economy (MKE, Korea). We thank the Tanaka Kikinzoku Kogyo K.K. for comments on the usage of palladium.

Received: May 21, 2014

Revised: July 26, 2014

Published online: September 2, 2014

- [1] a) R. M. Sutherland, J. A. McCredie, W. R. Inch, *J. Natl. Cancer Inst.* **1971**, *46*, 113; b) S. Kale, S. Biermann, C. Edwards, C. Tarnowski, M. Morris, M. W. Long, *Nat. Biotechnol.* **2000**, *18*, 954; c) J. Friedrich, C. Seidel, R. Ebner, L. A. Kunz-Schughart, *Nat. Protoc.* **2009**, *4*, 309; d) J. M. Kelm, M. Fussenegger, *Adv. Drug Del. Rev.* **2010**, *62*, 753; e) J. Lee, M. Sato, H. Kim, J. Mochida, *Eur. Cells and Mater.* **2011**, *22*, 275; f) S. H. Bhang, S. Lee, J.-Y. Shin, T.-J. Lee, B.-S. Kim, *Tissue Eng. Part A* **2012**, *18*, 2138; g) S. H. Bhang, S.-W. Cho, W.-G. La, T.-J. Lee, H. S. Yang, A.-Y. Sun, S.-H. Baek, J.-W. Rhie, B.-S. Kim, *Biomaterials* **2011**, *32*, 2734.
- [2] a) F. Pampaloni, E. G. Reynaud, E. H. Stelzer, *Nat. Rev. Mol. Cell Biol.* **2007**, *8*, 839; b) P. J. Tofilon, N. Buckley, D. F. Deen, *Science* **1984**, *226*, 862; c) S. F. Wong, D. Y. No, Y. Y. Choi, D. S. Kim, B. G. Chung, S.-H. Lee, *Biomaterials* **2011**, *32*, 8087; d) T. J. Bartosh, J. H. Ylöstalo, A. Mohammadipoor, N. Bazhanov, K. Coble, K. Claypool, R. H. Lee, H. Choi, D. J. Prockop, *Proc. Natl. Acad. Sci. U. S. A.* **2010**, *107*, 13724; e) J. E. Frith, B. Thomson, P. G. Genever, *Tissue Eng. Part C Methods* **2009**, *16*, 735.
- [3] S. Nori, Y. Okada, A. Yasuda, O. Tsuji, Y. Takahashi, Y. Kobayashi, K. Fujiyoshi, M. Koike, Y. Uchiyama, E. Ikeda, *Proc. Natl. Acad. Sci.* **2011**, *108*, 16825.
- [4] a) A. Y. Hsiao, Y.-S. Torisawa, Y.-C. Tung, S. Sud, R. S. Taichman, K. J. Pienta, S. Takayama, *Biomaterials* **2009**, *30*, 3020; b) Y.-S. Torisawa, A. Takagi, Y. Nashimoto, T. Yasukawa, H. Shiku, T. Matsue, *Biomaterials* **2007**, *28*, 559; c) C. M. Brophy, J. L. Luebke-Wheeler, B. P. Amiot, H. Khan, R. P. Rimmel, P. Rinaldo, S. L. Nyberg, *Hepatology* **2009**, *49*, 578.
- [5] G. Yirme, M. Amit, I. Laevsky, S. Osenberg, J. Itskovitz-Eldor, *Stem Cells Dev.* **2008**, *17*, 1227.
- [6] R. Glicklis, J. C. Merchuk, S. Cohen, *Biotechnol. Bioeng.* **2004**, *86*, 672.
- [7] J. M. Karp, J. Yeh, G. Eng, J. Fukuda, J. Blumling, K.-Y. Suh, J. Cheng, A. Mahdavi, J. Borenstein, R. Langer, *Lab Chip* **2007**, *7*, 786.
- [8] a) T. Sun, L. Feng, X. Gao, L. Jiang, *Acc. Chem. Res.* **2005**, *38*, 644; b) B. Bhushan, M. Nosonovsky, Y. C. Jung, *J. R. Soc. Interface* **2007**, *4*, 643; c) A. K. Brun-Graeppi, C. Richard, M. Bessodes, D. Scherman, O.-W. Merten, *Prog. Polym. Sci.* **2010**, *35*, 1311; d) T. Sun, G. Qing, *Adv. Mater.* **2011**, *23*, H57; e) X. Liu, Y. Liang, F. Zhou, W. Liu, *Soft Matter* **2012**, *8*, 2070; f) L. Cao, A. K. Jones, V. K. Sikka, J. Wu, D. Gao, *Langmuir* **2009**, *25*, 12444; g) N. J. Shirtcliffe, G. McHale, M. I. Newton, Y. Zhang, *ACS Appl. Mater. Interfaces* **2009**, *1*, 1316; h) J. R. Dorvee, A. M. Derfus, S. N. Bhatia, M. J. Sailor, *Nat. Mater.* **2004**, *3*, 896; i) X. Song, J. Zhai, Y. Wang, L. Jiang, *J. Phys. Chem. B* **2005**, *109*, 4048.
- [9] a) X. Feng, L. Jiang, *Adv. Mater.* **2006**, *18*, 3063; b) N. J. Shirtcliffe, G. McHale, M. I. Newton, C. C. Perry, F. B. Pyatt, *Appl. Phys. Lett.* **2006**, *89*, 104106; c) D. Tian, Q. Chen, F. Q. Nie, J. Xu, Y. Song, L. Jiang, *Adv. Mater.* **2009**, *21*, 3744.
- [10] a) P. S. Stayton, T. Shimoboji, C. Long, A. Chilkoti, G. Ghen, J. M. Harris, A. S. Hoffman, *Nature* **1995**, *378*, 472; b) C. Li, Y. Zhang, J. Ju, F. Cheng, M. Liu, L. Jiang, Y. Yu, *Adv. Funct. Mater.* **2012**, *22*, 760.
- [11] Z. Cheng, L. Feng, L. Jiang, *Adv. Funct. Mater.* **2008**, *18*, 3219.
- [12] C. Li, F. Cheng, J.-a. Lv, Y. Zhao, M. Liu, L. Jiang, Y. Yu, *Soft Matter* **2012**, *8*, 3730.
- [13] J. Wang, J. Hu, Y. Wen, Y. Song, L. Jiang, *Chem. Mater.* **2006**, *18*, 4984.
- [14] J. Seo, S. Lee, H. Han, H. B. Jung, J. Hong, G. Song, S. M. Cho, C. Park, W. Lee, T. Lee, *Adv. Mater.* **2013**, *25*, 4139.
- [15] F. A. Lewis, *The Palladium-Hydrogen System*, Academic Press, London, **1967**.
- [16] A. B. D. Cassie, S. Baxter, *Trans. Faraday Soc.* **1944**, *40*, 546.
- [17] a) T.-S. Wong, C.-M. Ho, *Langmuir* **2009**, *25*, 12851; b) C. Extrand, *Langmuir* **2002**, *18*, 7991; c) M. Dawood, H. Zheng, N. Kurniawan, K. Leong, Y. Foo, R. Rajagopalan, S. Khan, W. Choi, *Soft Matter* **2012**, *8*, 3549; d) C. Dorrer, J. Rühle, *Langmuir* **2007**, *23*, 3179.
- [18] S. M. Kang, I. You, W. K. Cho, H. K. Shon, T. G. Lee, I. S. Choi, J. M. Karp, H. Lee, *Angew. Chem., Int. Ed.* **2010**, *49*, 9401.
- [19] D. Quéré, *Annu. Rev. Mater. Res.* **2005**, *38*, 644.
- [20] D. Shweiki, M. Neeman, A. Itin, E. Keshet, *Proc. Natl. Acad. Sci.* **1995**, *92*, 768.
- [21] A. Guaccio, V. Guarino, M. A. A. Perez, V. Cirillo, P. A. Netti, L. Ambrosio, *Biotechnol. Bioeng.* **2011**, *108*, 1965.
- [22] J.-P. Piret, D. Mottet, M. Raes, C. Michiels, *Biochem. Pharmacol.* **2002**, *64*, 889.
- [23] G. L. Semenza, *Nat. Rev. Cancer* **2003**, *3*, 721.
- [24] M. Calvani, A. Rapisarda, B. Uranchimeg, R. H. Shoemaker, G. Melillo, *Blood* **2006**, *107*, 2705.
- [25] a) A. Petsi, V. Burganos, *Phys. Rev. E* **2008**, *78*, 036324; b) I. Sandu, C. T. Fleaca, *J. Colloid Interface Sci.* **2011**, *358*, 621.